Supplemental Figure 1. Long-term t-PDF expression does not induce sustained desensitization. 48 hours after co-transfection with 5 ng CRE-luc reporter, 2 ng PDFR, and the indicated t-PDF isoforms, HEK293 cells were exposed to saturating 1 μM soluble amidated PDF for four hours before luciferase assay. The TM-ML and TM-LL isoforms are identical to t-PDF-ML and t-PDF-LL except that the GPI targeting sequence has been replaced with the transmembrane domain of the human herpes simplex virus Type 1 glycoprotein C (WVGIGIGVLAAGVLVVTAIVYVV). There is no systematic effect of the pre-existing extent of PDFR activation induced by co-expressed t-PDF ligand on the cAMP level achieved by activation with saturating concentration of soluble PDF. Regardless of the extent of pre-existing PDFR activation—e.g., compare highly active TM-LL and inert SCR—the final cAMP level induced by applying saturating soluble PDF is the same. This indicates that t-PDF expression is not inducing substantial sustained desensitization of PDFR, which would reduce the availability of activatible PDFR and thus decrease the response to soluble PDF. Bars represent averages and s.e.m. of three duplicate wells. Similar results were obtained in an independent repeat experiment (data not shown).

Supplemental Figure 2. Absence of trans-activation of PDFR by t-PDF in tissue culture cells. (A) HEK293 cells were plated in 96 well plates, cultured 24h and then transfected with PDFR and CRE-LUC reporter. Twenty-four hours after transfection, 10000 cells transfected overnight with t-PDF-ML or empty vector were added per well. Twenty-four hours following cell addition, soluble PDF was added (1uM, 6h) into a subset of wells to confirm the presence of functional PDFR. PDFR is not activated by t-PDF expressed on the surface of the separate population of cells added to the well. (B)

Under the same conditions, in parallel wells, ELISA was performed to confirm the expression of t-PDF-ML. (n = 12 wells per condition; representative of two independent experiments).

Supplemental Figure 3. Immunofluorescence detection of epitope-tagged t-PDF expressed *in vivo* in circadian clock neurons. Whole-mount fly brains were fixed, permeabilized, and processed for anti-Myc + anti-PDF immunofluorescence using mouse anti-Myc and rabbit anti-PDF primary antibodies, using a previously described double-staining protocol[26], and imaged with confocal microscopy. t-PDF-ML is expressed in LN_Vs using *pdf-GAL4* driver and detected *via* the c-Myc epitope tag in the linker domain. Expression is greater in animals homozygous for both the *pdf-GAL4* and *UAS-t-PDF-ML* transgenes than in heterozygotes. Because the tissue has been detergent permeabilized, both surface and intracellular pools of t-PDF-ML within the secretory pathway are visualized.

Supplemental Figure 4. Immunofluorescence detection of GFP and PDF. Adult male brains with *UAS-nlsGFP* expression driven by *cry16-GAL4* or *cry24-GAL4* were co-immunostained with antiGFP(green) and antiPDF (red) and imaged using confocal microscopy. With both *cry16-GAL4* and *cry24-GAL4*, nlsGFP is detected in the small LNvs, large LNvs, and can also be detected in ring neurons of the central complex (both in the nuclei and also in the projections to the ring, as the nuclear localization sequence is apparently not 100% effective at keeping GFP solely in the nuclei).

Supplemental Figure 5. Immunofluorescence detection of GFP and Repo. Adult male brains with *UAS-nlsGFP* expression driven by *cry16-GAL4* or *cry24-GAL4* were co-immunostained with antiGFP(green) and antiRepo (red)—a glial marker—and imaged

using confocal microscopy. While many of the GFP-positive cells are glial in *cry16-GAL4* animals, none of them are glial in *cry24-GAL4* brains.

Supplemental Figure 6. Immunofluorescence detection of GFP and PDP1. Adult male brains with *UAS-nlsGFP* expression driven by *cry16-GAL4* or *cry24-GAL4* were co-immunostained with antiGFP(green) and antiPDP1 (red)—a clock neuron marker—and imaged using confocal microscopy. Both *cry16-GAL4* and *cry24-GAL4* drive GFP expression in DN1a, DN2, and subsets of DN1p clock neurons. However, the number of GFP positive cells in *cry16 > nlsGFP* animals is more variable than the number of GFP positive cells in *cry24 > nlsGFP* animals. In *cry24 > nlsGFP* there are almost always four or five PDP1- and GFP-positive DN1p clock neurons, while in *cry16 > nlsGFP* the number varies from two to six. Counts of PDP1- and GFP-positive DN1p clock neurons in six brain hemispheres of *cry24-GAL4* flies were 4, 5, 5, 4, 4, and 3; counts of PDP1- and GFP-positive DN1p clock neurons in fourteen brain hemispheres of *cry16-GAL4* flies were 4, 6, 4, 2, 4, 5, 6, 6, 6, 5, 3, 5, 5, 2.

Supplemental Figure 7. Immunofluorescence detection of GFP and PDP1. Adult male brains with *UAS-nlsGFP* expression driven by *cry16-GAL4* or *cry24-GAL4* were co-immunostained with antiGFP(green) and antiPDP1 (red)—a clock neuron marker—and imaged using confocal microscopy. Both *cry16-GAL4* and *cry24-GAL4* drive GFP expression in all five LN_D clock neurons and an adjacent sixth PDP1-negative cell, and in two or three large DN3s.

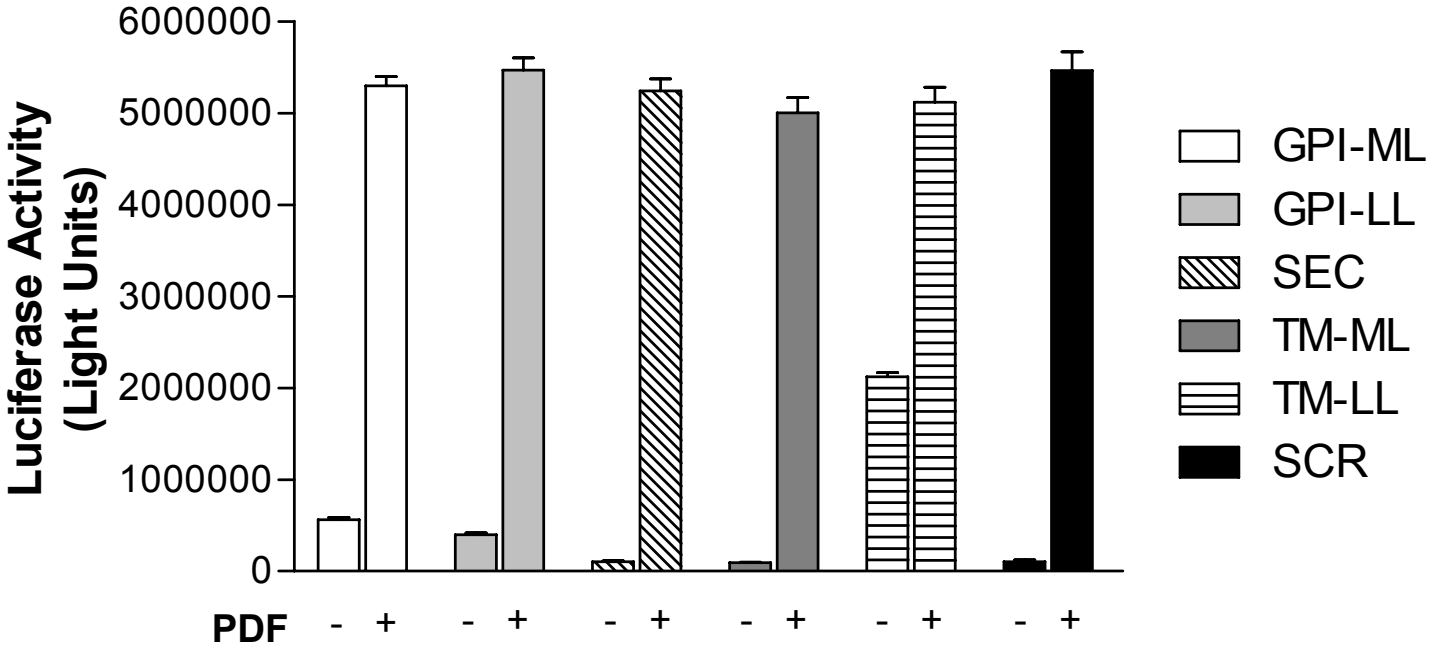

Choi et al., Supplemental Figure 1

A

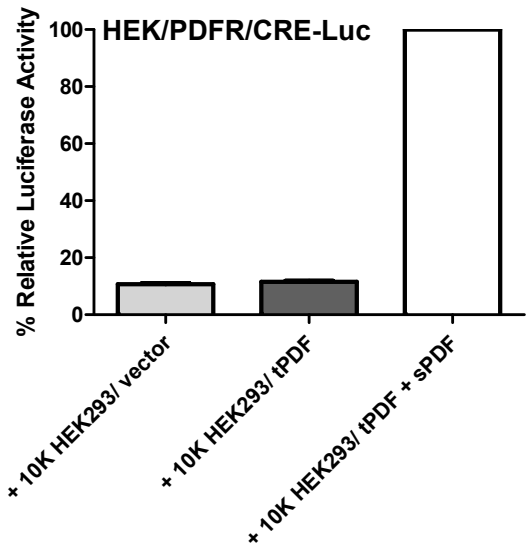

B

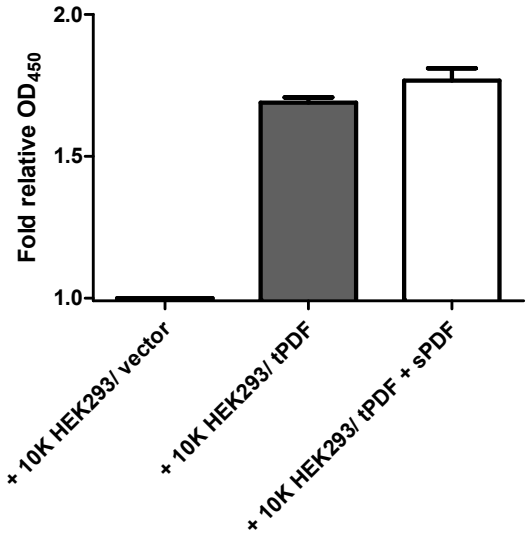

Choi et al., Supplemental Figure 2

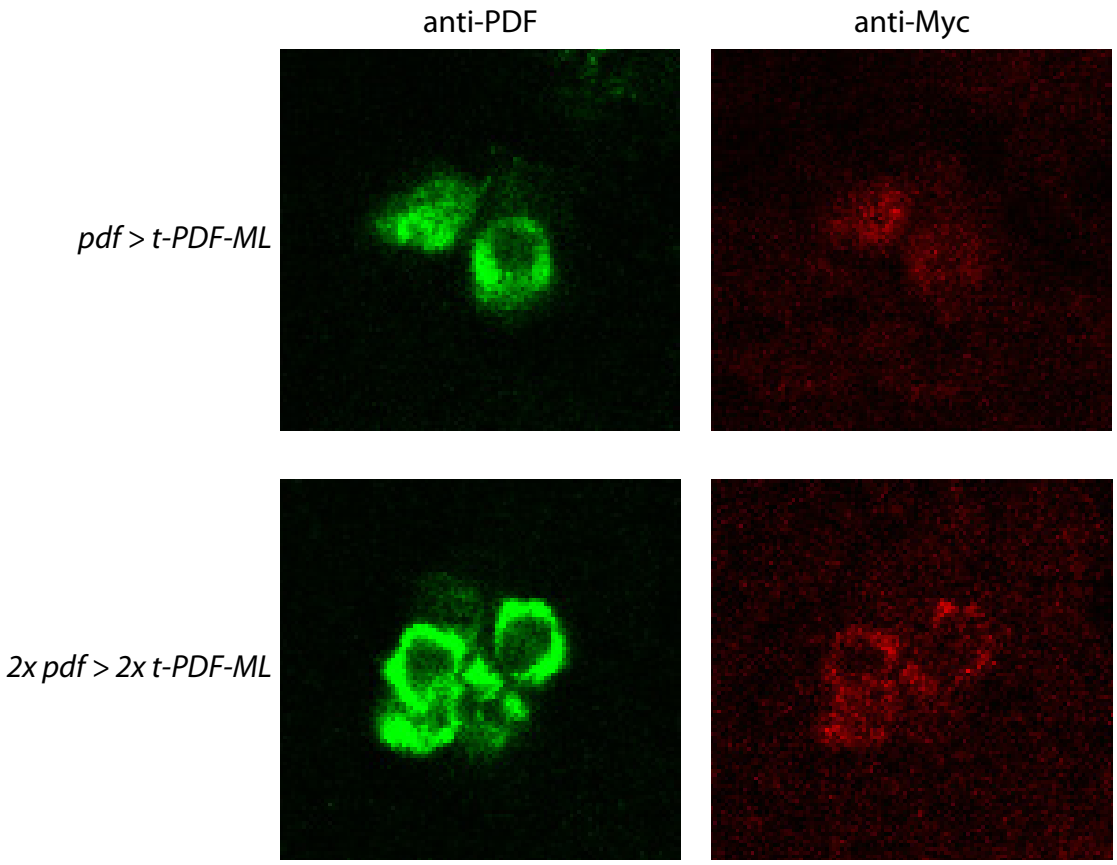

Choi et al., Supplemental Figure 3

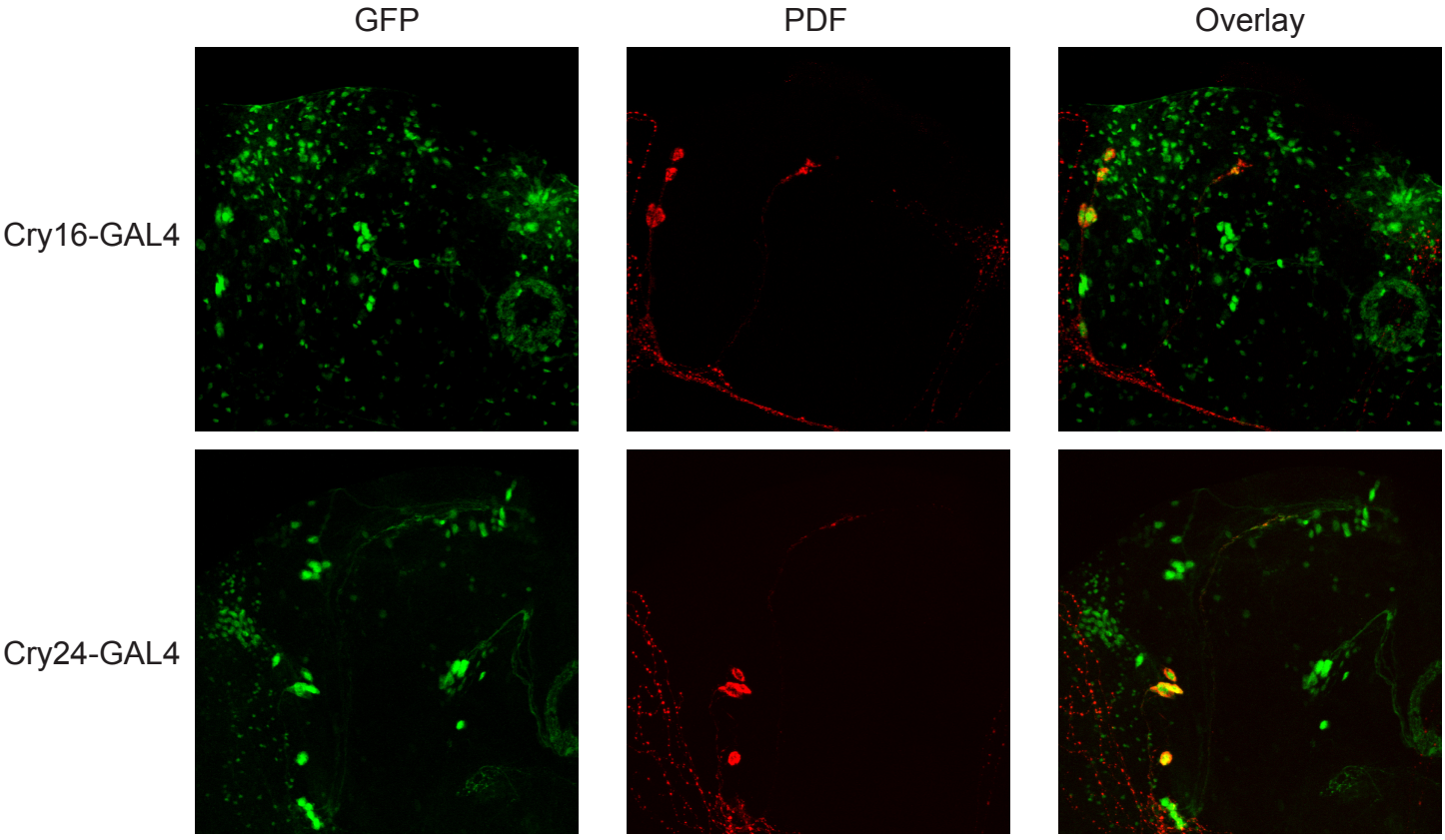

Choi et al., Supplemental Figure 4

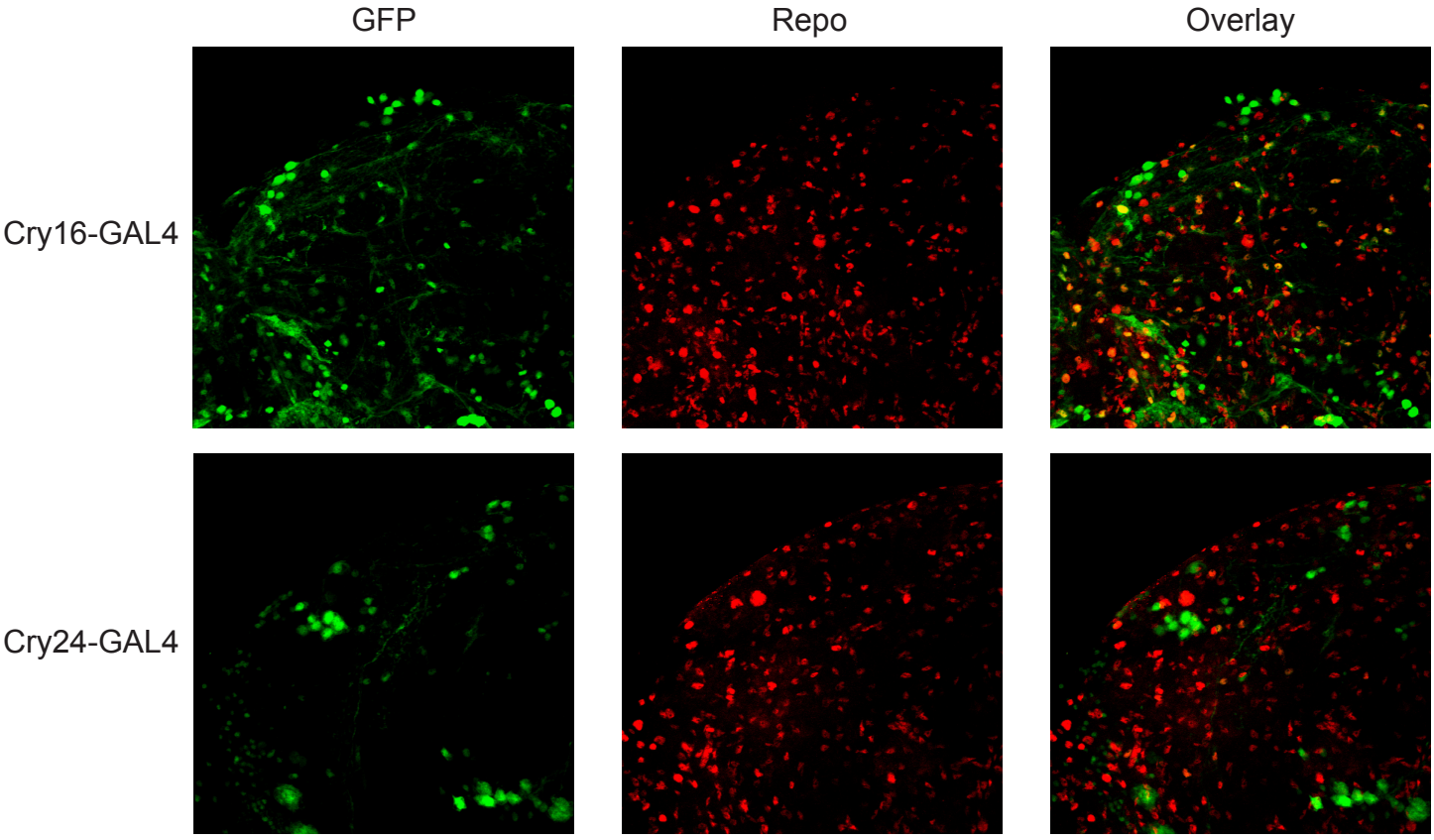

Choi et al., Supplemental Figure 5

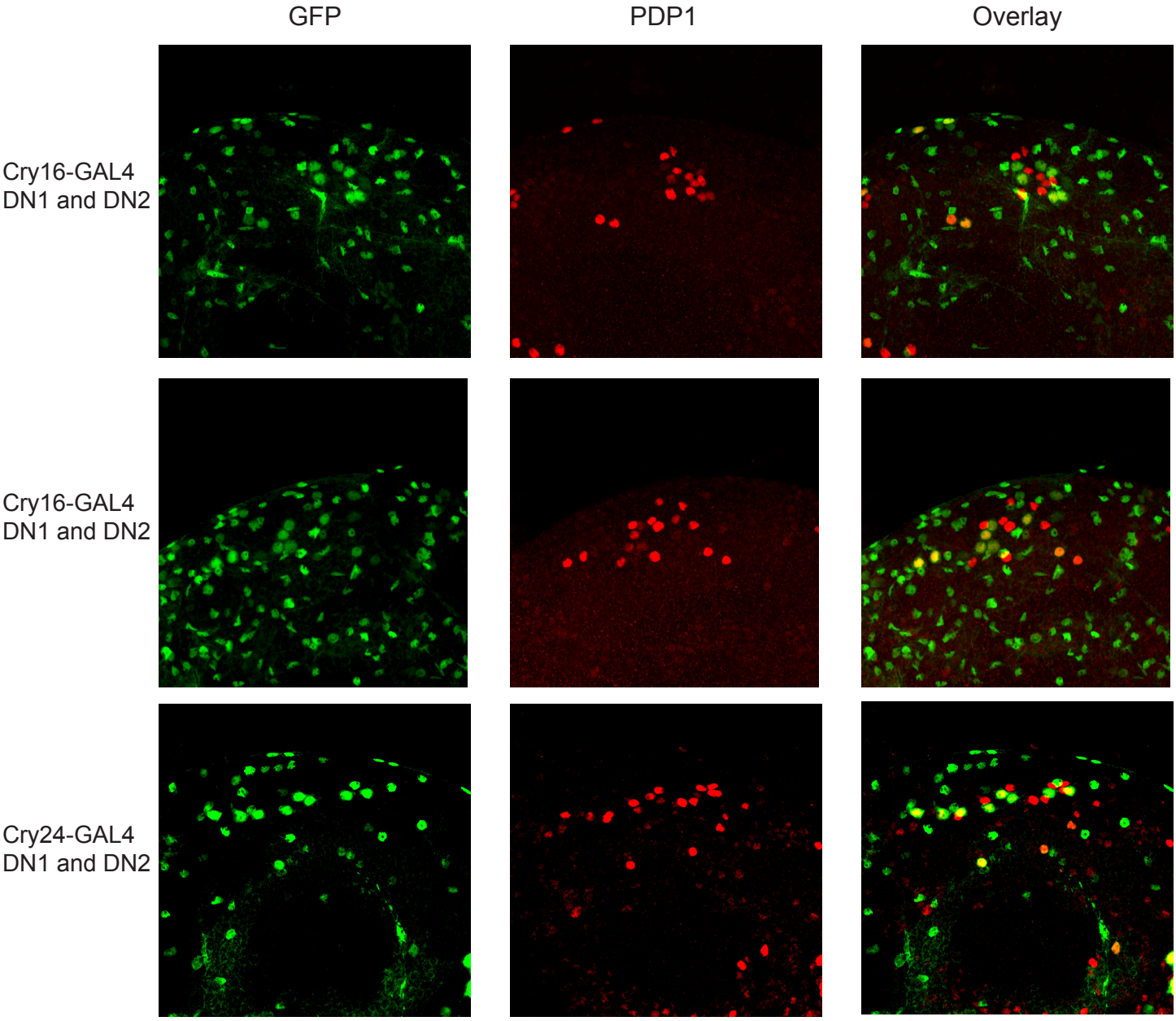

Choi et al., Supplemental Figure 6

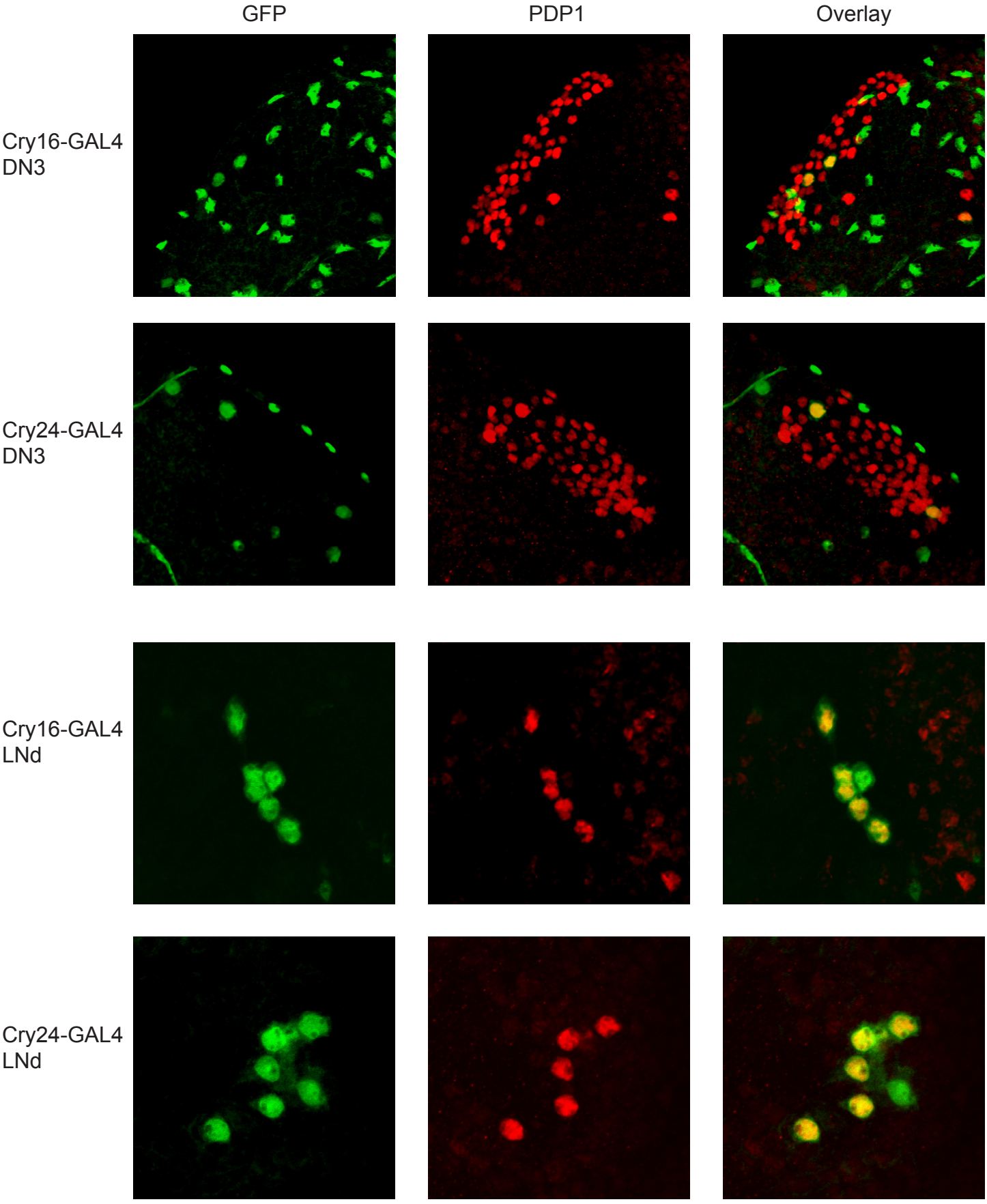

Choi et al., Supplemental Figure 7

Supplemental Table. Tethered-PDF expression in various subsets of neurons. t-PDF-ML was expressed in various subsets of Drosophila cells under different cell specific GAL4 drivers and their circadian locomotor behavior in constant darkness were characterized. GAL4, cell specific GAL4 driver used; UAS, UAS transgene expressed by the GAL4 driver; %A, percentage of arrhythmic flies; %C, percentage of complex rhythmic flies; %R, percentage of rhythmic flies; n, number of individual animals of the genotype; $\mathbf{X^2}$, Chi-square test (*, P<0.05; **, p<0.001; ***, P<0.0001; n.s., not significantly different).

GAL4	UAS	%A	%C	%R	n	X^2	Expression pattern	Reference
C232	t-MrVIa	2	0	98	62		Central complex, R3 and R4d ring neuorns of ellipsoid body	[1, 2]
C232	t-PDF-ML(M2a)	0	0	100	27	n.s.		
C232	t-PDF-ML(M3a)	0	0	100	32	n.s.		
C232	t-PDF-ML(M2a,M3a)	0	3	97	32	n.s.		
121Y	t-MrVIa	3	2	95	63		Pars intercerebralis and beta and gamma lobe of mushroom body	[3, 4]
121Y	t-PDF-ML(M2a)	18	0	82	28	n.s.		
121Y	t-PDF-ML(M2aM3a)	0	10	90	30	n.s.		
104Y	none	4	7	88	27	n.s.	Fan shaped body, cells rimming the optic lobe neurons, SOG and smaller number of neurons diffused around the brain	[5, 6]
104Y	t-MrVIa	6	0	94	31			
104Y	t-PDF-ML(M2a)	0	0	100	31	n.s.		

104Y	t-PDF-ML(M6a)	3	0	97	31	n.s.		
104Y	t-PDF-ML(M2aM3a)	0	3	97	30	n.s.		
C547	t-MrVIa	0	0	100	32		Pars intercerebralis and R2 and medial R4 neurons of ellipsoid body	[7]
C547	t-PDF-ML(M2aM3a)	0	0	100	32	n.s.		
30Y	t-MrVIa	0	0	100	32		Mushroom body, lateral protocerebrum, antennal lobe, subesophageal ganglion, optic lobe.	[8]
30Y	t-PDF-ML(M2aM3a)	3	0	97	32	n.s.		
50Y	t-MrVIa	59	0	41	32		Subset of neurons in pars intercerebralis	[9]
50Y	t-PDF-ML(M2aM3a)	13	0	87	23	***		
C687	t-MrVIa	3	0	97	31		Subset of neurons in pars intercerebralis	[9]
C687	t-PDF-ML(M2aM3a)	0	0	100	25	n.s.		
C767	t-MrVIa	22	0	78	32		Subset of neurons in pars intercerebralis	[9]
C767	t-PDF-ML(M2aM3a)	6	0	94	32			

EB1	t-MrVIa	0	0	100	15		Ellipsoid body	[10]
EB1	t-PDF-ML(M2aM3a)	0	0	100	13	n.s.		
Feb170	t-MrVIa	0	0	100	32		R4m neurons of Ellipsoid body	[11]
Feb170	t-PDF-ML(M2a)					n.s.		
Feb170	t-PDF-ML(M2aM3a)	0	0	100	32	n.s.		
J183	t-PDF-SCR(A2)	20	0	80	15		Fan shaped body, restricted subsets of the mushroom body, scattered cells in the optic lobes	[12, 13]
J183	t-PDF-ML(M2aM3a)	0	0	100	26	n.s.		
Mj126a	t-PDF-SCR(A2)	23	0	77	22			[12]
Mj126a	t-PDF-ML(M2aM3a)	0	0	100	27	**		
OK348	t-MrVIa	4	0	96	28		Fan shaped body	[12, 13]
OK348	t-PDF-ML(M2aM3a)	10	0	90	29	n.s.		
repo(III)	t-PDF-SCR(A2)	0	0	100	29		Glial cells	[14]
repo(III)	t-PDF-ML(M2aM3a)	0	0	100	30	n.s.		
repo(II)	t-PDF-SCR(A2)	4	0	96	27		Glial cells	[14]

repo(II)	t-PDF-ML(M2a)	8	0	92	12	n.s.		
repo(II)	t-PDF-ML(M2aM3a)	2	0	98	44	n.s.		
MZ1366	t-MrVIa	0	0	100	39		Neurons of the brain including neurosecretory neurons that project to the dorsolateral posterior brain	[15]
MZ1366	t-PDF-LL(M1b)	0	0	100	15	n.s.		
MZ1366	t-PDF-ML(M2a)	6	0	94	31	n.s.		
MZ1366	t-PDF-ML(M6a)	8	0	92	40	n.s.		
MZ1525	t-MrVIa	10	0	90	10		Neurons of the brain including neurosecretory neurons that project to the dorsolateral posterior brain	[15]
MZ1525	t-PDF-ML(M2a)	5	3	92	38	n.s.		
pdfGAL4;pdf^{WT}	t-MrVIa	7	0	93	43		Large and small LN_vs in a pdf-wildtype background	[16]
pdfGAL4;pdf^{WT}	t-PDF-SCR(A2)	8	0	92	25	n.s.		
pdfGAL4;pdf^{WT}	t-PDF-ML(M2a)	21	0	79	78	*		
pdfGAL4;pdf^{WT}	t-PDF-ML(M3a)	20	0	80	30	n.s.		
pdfGAL4;pdf^{WT}	t-PDF-ML(M6a)	25	0	75	56	**		
pdfGAL4;pdf^{WT}	t-PDF-ML(M2aM3a)	13	0	87	24	n.s.		
pdfGAL4;pdf^{WT}	t-PDF-ML(M2aM6a)	26	0	74	27	*		
pdfGAL4;pdf^{WT}	t-PDF-ML(M3aM6a)	10	0	90	30	n.s.		
pdfGAL4;pdf^{01}	t-MrVIa	63	0	37	40		Large and small LN_vs in a pdf-null mutation background	[16]
pdfGAL4;pdf^{01}	t-PDF-SCR(A2)	48	0	52	27	n.s.		

pdfGAL4;pdf^{01}	t-PDF-ML(M2a)	46	0	54	52	n.s.
pdfGAL4;pdf^{01}	t-PDF-ML(M3a)	48	0	52	31	n.s.
pdfGAL4;pdf^{01}	t-PDF-ML(M6a)	47	3	50	74	n.s.
pdfGAL4;pdf^{01}	t-PDF-ML(M3aM6a)	61	0	39	18	n.s.

*, P<0.05; **, p<0.001; ***, P<0.0001; n.s., not significantly different

REFERENCES

1. Besson, M., and Martin, J.R. (2005). Centrophobism/thigmotaxis, a new role for the mushroom bodies in Drosophila. J Neurobiol *62*, 386-396.
2. O'Dell, K.M., Armstrong, J.D., Yang, M.Y., and Kaiser, K. (1995). Functional dissection of the Drosophila mushroom bodies by selective feminization of genetically defined subcompartments. Neuron *15*, 55-61.
3. Belgacem, Y.H., and Martin, J.R. (2002). Neuroendocrine control of a sexually dimorphic behavior by a few neurons of the pars intercerebralis in Drosophila. Proc Natl Acad Sci U S A *99*, 15154-15158.
4. Gatti, S., Ferveur, J.F., and Martin, J.R. (2000). Genetic identification of neurons controlling a sexually dimorphic behaviour. Curr Biol *10*, 667-670.
5. Joiner, W.J., Crocker, A., White, B.H., and Sehgal, A. (2006). Sleep in Drosophila is regulated by adult mushroom bodies. Nature *441*, 757-760.
6. Liu, G., Seiler, H., Wen, A., Zars, T., Ito, K., Wolf, R., Heisenberg, M., and Liu, L. (2006). Distinct memory traces for two visual features in the Drosophila brain. Nature *439*, 551-556.
7. Renn, S.C., Armstrong, J.D., Yang, M., Wang, Z., An, X., Kaiser, K., and Taghert, P.H. (1999). Genetic analysis of the Drosophila ellipsoid body neuropil: organization and development of the central complex. J Neurobiol *41*, 189-207.
8. Mehren, J.E., and Griffith, L.C. (2006). Cholinergic neurons mediate CaMKII-dependent enhancement of courtship suppression. Learn Mem *13*, 686-689.
9. Foltenyi, K., Greenspan, R.J., and Newport, J.W. (2007). Activation of EGFR and ERK by rhomboid signaling regulates the consolidation and maintenance of sleep in Drosophila. Nat Neurosci *10*, 1160-1167.
10. Wang, J., Zugates, C.T., Liang, I.H., Lee, C.H., and Lee, T. (2002). Drosophila Dscam is required for divergent segregation of sister branches and suppresses

ectopic bifurcation of axons. Neuron *33*, 559-571.

11. Wu, C.L., Xia, S., Fu, T.F., Wang, H., Chen, Y.H., Leong, D., Chiang, A.S., and Tully, T. (2007). Specific requirement of NMDA receptors for long-term memory consolidation in Drosophila ellipsoid body. Nat Neurosci *10*, 1578-1586.
12. Joiner, M.A., and Griffith, L.C. (1999). Mapping of the anatomical circuit of CaM kinase-dependent courtship conditioning in Drosophila. Learn Mem *6*, 177-192.
13. Sakai, T., and Kitamoto, T. (2006). Differential roles of two major brain structures, mushroom bodies and central complex, for Drosophila male courtship behavior. J Neurobiol *66*, 821-834.
14. Suh, J., and Jackson, F.R. (2007). Drosophila ebony activity is required in glia for the circadian regulation of locomotor activity. Neuron *55*, 435-447.
15. Helfrich-Forster, C., Tauber, M., Park, J.H., Muhlig-Versen, M., Schneuwly, S., and Hofbauer, A. (2000). Ectopic expression of the neuropeptide pigment-dispersing factor alters behavioral rhythms in Drosophila melanogaster. J Neurosci *20*, 3339-3353.
16. Renn, S.C., Park, J.H., Rosbash, M., Hall, J.C., and Taghert, P.H. (1999). A pdf neuropeptide gene mutation and ablation of PDF neurons each cause severe abnormalities of behavioral circadian rhythms in Drosophila. Cell *99*, 791-802.